THE ASTROPHYSICAL JOURNAL, 454:125–133, 1995 November 20

LOW-FREQUENCY CARBON RECOMBINATION LINES IN THE CENTRAL REGIONS OF THE GALAXY

W. C. ERICKSON[1]
University of Maryland, Astronomy Department, College Park, MD 20742
D. MCCONNELL
Australia Telescope National Facility, Locked Bag 194, Narrabri, NSW 2390, Australia
AND
K. R. ANANTHARAMAIAH
Raman Research Institute, Sadhashivangar, Bangalore 560080, India
Received 1995 February 2; accepted 1995 June 1

ABSTRACT

We have used the Parkes 64 m telescope to study low-frequency carbon recombination lines from the southern portion of the Galactic plane in a frequency band 4 MHz wide centered at 76.4 MHz. We have found a very large line-forming region that extends for approximately 40° in Galactic longitude from $l = 340°$ to $l = 20°$. The region is several degrees wide in latitude. From the variation of radial velocity and line width with Galactic longitude we obtain kinematic distances to the line-forming region in the range 0.5–4 kpc. This places the line-forming region in the Sagittarius and/or Scutum arms. We also find the lines approximately tangent to the Scutum arm at $l = 312°$. By observing the C441α, C555β, and C635γ lines, which all occur in the analyzed band, we estimate the variation of line strength with principal quantum number. This variation appears to be similar to that of the well-observed Perseus arm absorption in the direction of Cas A and suggests that a model for the Perseus arm line-forming region may be at least partially applicable to the Sagittarius/Scutum arm regions. The most likely sites for the formation of these lines are the cold neutral H I concentrations in the interstellar medium. We have also searched the data for other lines and, in particular, we find no trace of hydrogen recombination lines.

Subject headings: Galaxy: structure — radio lines: ISM

1. INTRODUCTION

Low-frequency carbon recombination lines were first discovered in the direction of Cas A (Konovalenko & Sodin 1980; Blake, Crutcher, & Watson 1980), and this is the direction in which the lines have been most extensively studied. At frequencies below 150 MHz the lines are found to be in absorption; at higher frequencies they are in emission (Payne, Anantharamaiah, & Erickson 1989, hereafter PAE89). These lines have proven to be very useful diagnostics of the physical conditions, such as temperature, density, level of ionization, heating, and cooling in the Perseus arm clouds where they are formed. Studies of the lines have also shed light on new processes, such as dielectronic recombination of carbon in warm H I clouds as suggested by Watson, Western, & Christiansen (1980), the limiting sizes of Rydberg atoms as a result of neutral interactions, and modifications to the boundary conditions required for calculating the population of high quantum number states (Payne, Anantharamaiah, & Erickson 1994, hereafter PAE94).

Until now, these recombination lines have only been detected in about half a dozen directions, all of them near the Galactic plane (Konovalenko 1984; Anantharamaiah, Payne, & Erickson 1988; Golynkin & Konovalenko 1990). The general picture that has emerged, especially from the detailed observations toward Cas A, is that the lines are associated with H I. However, there are some counterexamples in which the lines appear to be associated with cold molecular clouds (Konovalenko 1984; Golynkin & Konovalenko 1990). Since H I and molecular clouds are widely distributed in the Galaxy, it is somewhat surprising that there have been only a few detections of low-frequency carbon lines in spite of several searches (e.g., Anantharamaiah et al. 1988). It is not clear whether this is the result of some instrumental limitation, such as beam dilution, or specific physical conditions in the clouds. PAE94 have argued that the temperature of the clouds could be crucial in determining whether the carbon lines are detectable; colder clouds ($T < 50$ K) could be more easily detectable than the warmer ones. More searches and detections are clearly needed to answer some of the questions. Previous observations were all made with northern hemisphere telescopes, and most of the detections were in the northern hemisphere. A promising area to search for new detections is in the southern sky, especially the central regions of the Galaxy where the column densities of interstellar material tend to be large and where the Galactic background emission is intense, facilitating the detection of absorption lines. We have made an initial search in this region using the Parkes Telescope in New South Wales, Australia.

2. OBSERVATIONS

Our observations were made near 76 MHz with the Parkes Observatory 64 m telescope (latitude −33°). They utilized a special low-frequency feed that was constructed for this program and the ATNF 16384 channel autocorrelator. The feed consists of crossed dipoles in an open-sleeve, wide-band configuration, and it operates from 44 to 92 MHz. It is a copy of a similar one that was designed and constructed at NRAO–Green Bank and is based upon design data developed at Aero-

[1] Present address: University of Tasmania, Physics Department, GPO Box 252C, Hobart 7001, Tasmania, Australia.

space Corporation (Wong & King 1990). The telescope is not very efficiently illuminated by the feed, resulting in an aperture efficiency of only 25%. The half-power beamwidth of the telescope at 76 MHz was determined from scans of Cen A to be 4°.

After a preliminary study of the interference spectrum, we decided that 76 MHz would be an appropriate frequency for our initial observations. This band appeared to be relatively clear of interference late at night. The recombination lines strengthen at lower frequencies, but as the frequency decreases the interference levels generally increase and the angular resolution of the telescope becomes poorer. Thus, 76 MHz appeared to be a reasonable compromise frequency.

The wide-band antenna signals were preamplified using transistor amplifiers. Tunable bandpass filters of 4 MHz bandwidth were placed ahead of the amplifiers to protect them from strong interference at nearby frequencies. The amplifiers were highly linear and capable of handling quite strong interference without intermodulation, and they had noise figures of about 2.9 dB. Considering the filter losses, this translates to an excess receiver temperature of 360 K at the antenna terminals. The Galactic background radiation usually raised the system temperature to about 10^4 K, so the antenna noise greatly dominated the preamplifier noise in every case. In the control room, the signals were injected into a normal Parkes receiver setup.

The autocorrelator was partitioned into two 8192 channel sections, one for each polarization, and analyzed a total bandwidth of 4 MHz. The data were Hanning smoothed, resulting in 977 Hz frequency resolution or 3.83 km s^{-1} velocity resolution. No frequency or load switching was employed. The band to be analyzed was centered on the C441α transitions at 76.4529 MHz but covered a total of seven transitions from C438α to C444α. By averaging the data from the two polarizations and from all seven transitions we could, ideally, accumulate effective integration time at 14 times real time. In practice, interference or other problems forced us to discard a significant portion of the data, but we usually could accumulate effective integration time at 10–12 times real time. The lines are weak, with line-to-continuum ratios of about 10^{-3}, and 40–100 minutes of real time were generally required for a detection. The large number of autocorrelator channels was extremely beneficial for this project. It allowed easy recognition and excision of interference and also provided excellent baseline data between the lines, eliminating the need for switching.

The first observing session ran for seven nights commencing 1993 June 22; a second session of similar length began on 1994 March 29. Daytime observations were found to be practically impossible because of terrestrial interference, but between about 11 P.M. and 6 A.M. local time there was little interference external to the Observatory. However, there remained high interference levels generated by many different items of equipment at the Observatory, especially the Uninterruptable Power Supply (UPS) systems. This forced us to shut down the UPS systems and all nonessential equipment. During our observations, we turned off the main power to the Observatory and operated only the telescope drives and the control computer using a local diesel generator.

During the first observing session, we began observing particular directions deemed to be the most likely line production directions because they contained strong background radiation, H I and molecular gas, H II regions, and the like. After some nights of observing, it became apparent that there existed a widespread line production region, one not confined to particular directions but lying along the Galactic plane for about 40° in longitude. During the second observing session, we systematically explored the angular extent of this region. In many cases fields observed in the second session were centered on coordinates that were only a small fraction of a beamwidth different from those of the first session. The data were in reasonable agreement between the two observing sessions.

3. DATA PROCESSING

The autocorrelation data were Fourier transformed, Hanning smoothed, and averaged over the observation period, which was typically about 3000 s. The averaged data were then processed by a special program that selects 256-channel segments of the data (± 240 km s^{-1} in velocity) centered on each of the lines that fall within the passband. To avoid being perturbed by large interference signals, these data were clipped and then displayed as shown in Figure 1. The data quality was then assessed visually and, frequently, some of the lines or polarizations were discarded if they appeared to be so badly corrupted by interference that they would not contribute usefully to the average. The remaining data were then averaged to obtain a profile as shown in the bottom panel of Figure 1. In addition to the seven α-lines, the 4 MHz bandpass contained 10 of the β-lines and 11 of the γ-lines.

Multiple observations of the same field were then averaged together, a third-order polynomial was fitted to the baseline, and the largest negative response within a 50 km s^{-1} interval centered on the expected line velocity was fitted with a Gaussian. If the largest response was positive, no fit was made, since under normal interstellar conditions the carbon recombination lines at the frequency are expected to be in absorption (PAE89). Many examples of the line profiles and their fitted Gaussians are displayed in Figure 2.

Some parameter was needed to estimate the reliability of the detection or nondetection of lines. Since most of the reliably detected lines were found to be about 20 km s^{-1} wide, the data from -240 km s^{-1} to $+240$ km s^{-1} were averaged in 20 km s^{-1} bins (excluding a 50 km s^{-1} interval at the expected line velocity). The standard deviation of these averaged data was calculated. This deviation should provide some measure of the fluctuations to be expected in the data when they are averaged over a typical line width, i.e., a measure of the baseline fluctuations. In the case of nondetection, it provides a measure of the level at which a line should have been detectable while, in the case of detection, it provides a measure of the reliability of the detection.

Upon cursory inspection, some of the profiles appeared to be asymmetrical, but fits with two Gaussians were not significantly better than fits with a single Gaussian, so the latter was used in every case.

4. RESULTS

4.1. *Line Parameters*

Some 50 fields were observed with varying sensitivities. In some of the fields our effective sensitivity was marginal for detection of lines at a T_L/T_{sys} level of about 10^{-3}. Several fields were observed with sensitivities similar to those which yielded detections, but no lines were observed. About 30 fields yielded positive detections, but two of these detections are not new (G000.0+0.0 and G016.9+0.8, e.g., M16; see Anantharamaiah et al. 1988), and in many cases the fields overlap within a fraction of a beamwidth, so many of the new detections are not unique. Most fields from $l = 340°$ to $l = 20°$ with $|b| \leq 4°$

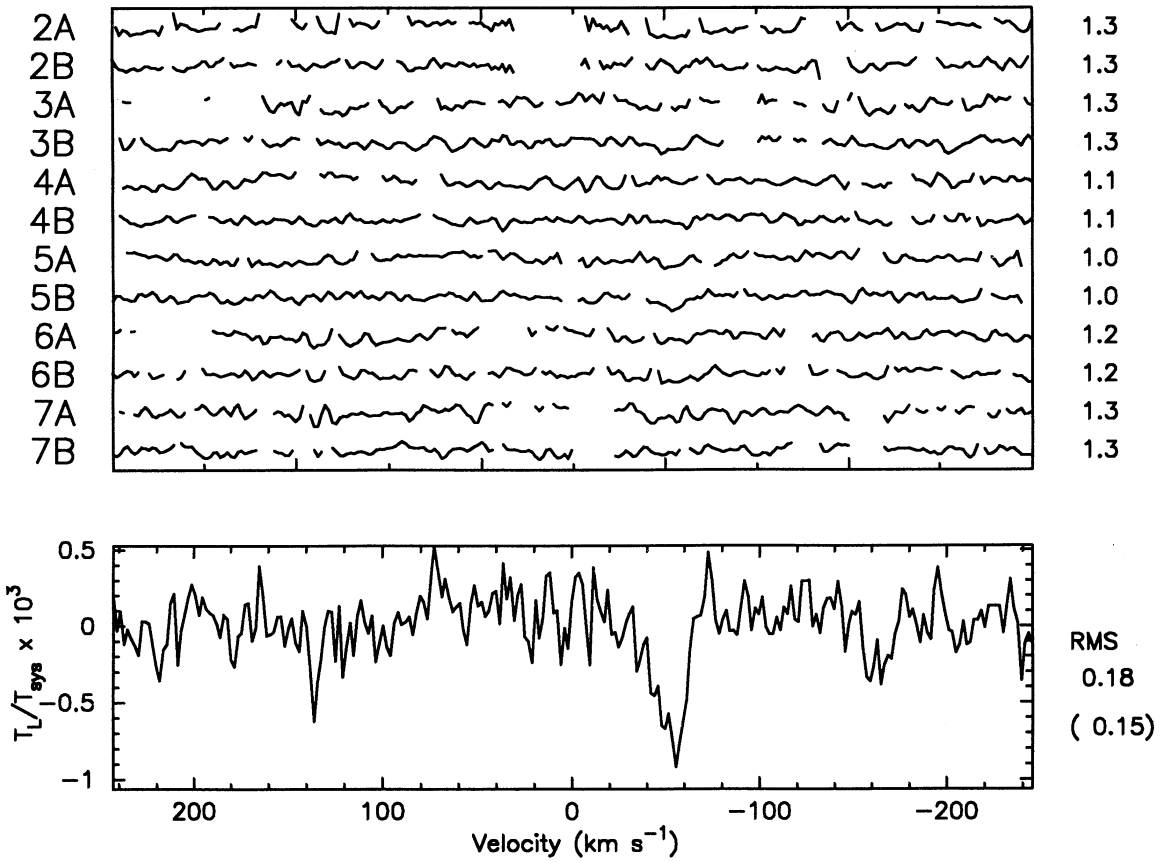

FIG. 1.—The data from G312+0.0 are used as an example of the method of summing the various line components. The seven line components in the two polarizations are listed and displayed in the top panel. (In this example, lines 1A and 1B were excluded because of interference.) The averaged spectrum is shown in the lower panel. On the right side, the measured and predicted rms noise levels are given.

yielded α-line detections. β-lines were detected in nearly all the fields that yielded α-line detections.

Table 1 summarizes the results of the fitting procedure and the estimated line parameters for all of the observed directions. Column (1) identifies the observed field. Column (2) is the total length of the observation (telescope time) in thousands of seconds. Note that the effective integration time is more than 10 times this quantity, since up to seven transitions observed in two polarizations have been averaged. Column (3) is the total system temperature, T_{sys}, as measured relative to a noise diode. It is essentially equal to the Galactic background temperature. Columns (4)–(6) refer to the α-lines, and columns (7)–(9) refer to the β-lines. The line depth given in column (4) is the line temperature divided by the system temperature times 1000, i.e., $T_L/T_{sys} \times 10^3$. The number in parenthesis in column (4) gives the baseline fluctuation parameter that was discussed in the previous section, again in units of $T_L/T_{sys} \times 10^3$. For a reliable detection, the line depth given in column (4) should be 5–10 times this parameter. However, it is not possible to describe the complex baseline fluctuations by a single parameter, especially because many of the fluctuations are caused by interference and do not have a noiselike character. Therefore, this baseline parameter should be interpreted with caution. Sometimes an examination of the actual profile indicates that the detection is quite reliable even when the ratio of line depth to baseline parameter is only about five; on other occasions, the detection appears to be doubtful even if the ratio is higher. Whenever the detection is judged to be doubtful, a question mark is placed after column (4). Column (5) is the half-width of the Gaussian profile that was fitted to the line. Formal errors on the half-widths are given in parentheses following column (5). Half-widths of about 10 km s^{-1} or less may be erroneous; often they appear to have been caused by noise spikes superimposed upon a broader profile. *Half-widths greater than about 30 km s^{-1} should also be interpreted with caution; they may be caused by broad baseline fluctuations.* The α-line velocity with respect to the local standard of rest is given in column (6). Formal errors on the line velocities are about half the errors on the line width. The line velocity shows a smooth variation with Galactic longitude, presumably as a result of differential rotation. Generally, the fitted line represents the largest negative deflection within the ±240 km s^{-1} spectrum that was analyzed. When a spectrum shows no major deflections or several deflections of similar magnitude, no fitted parameters are given in columns (4)–(6). Columns (7)–(9) give similar parameters for the β-lines. β-lines which are narrower than the corresponding α-lines should be interpreted with caution since the β-lines, which arise from higher quantum levels, are expected to be at least as wide or wider than the α-lines. Such cases are identified by an exclamation point placed after column (7). However, since the observed α-lines are likely to have originated in a number of clouds within the beam area, the β-lines could be narrower if only a subset of these clouds contribute to the β-lines. Column (10) gives the near-kinematic distance to the line-forming region based upon the α-line velocities and the Galactic rotation model given by Burton (1988).

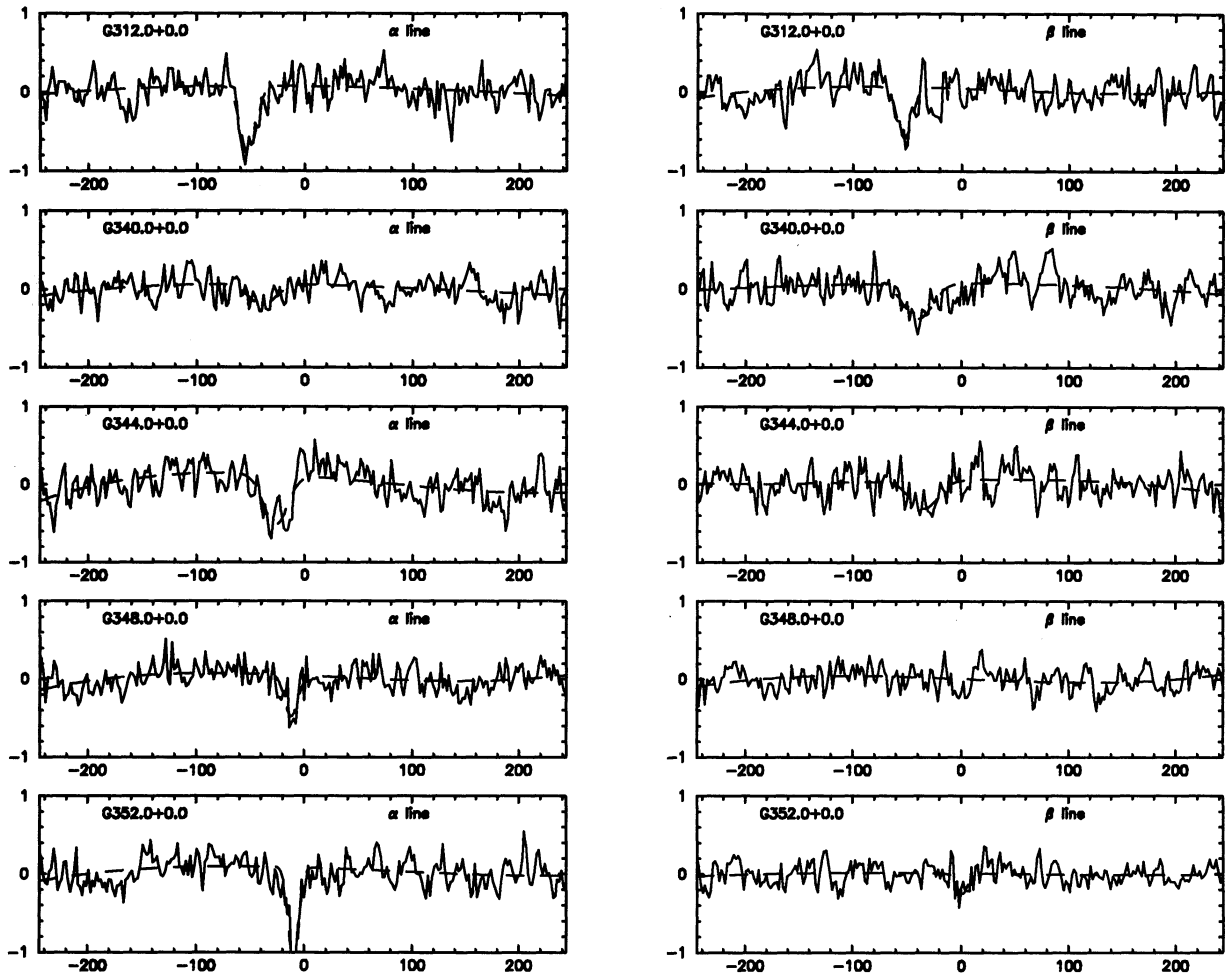

FIG. 2.—Examples of the observed line α- and β-line profiles. The abcissae are velocity in km s^{-1} with respect to the local standard of rest; the ordinates are the channel temperatures at each velocity in units of thousandths of the total system temperature. The characteristics of the fitted curves are in Table 1.

If the observed width of the lines is the result of Galactic rotation (see below), the kinematic distances are consistent with the gas being in the Sagittarius and/or Scutum arm regions.

All the line parameters should be interpreted with some caution because many of the fluctuations are caused by weak interference rather than Gaussian noise. The details of line widths, depths, and shapes depend upon the choice of clipping levels and upon the subjective choice of which line components were included or excluded from the average. No standard errors are quoted for the line parameters given in Table 1 because they would have very little meaning.

It may also be noted that the baseline fluctuation parameters from the β-lines are generally a bit lower than those for the α-lines. This is probably caused by the larger number of β-lines in the bandpass and, consequently, larger effective integration times. Thus, we may expect that the sensitivity for the detection of β-lines will be somewhat higher than that for α-lines. On the other hand, the β-lines are expected to be intrinsically weaker than the α-lines.

4.2. *Line Detections*

The first nine entries in Table 1 represent particular directions that are observed. Low-frequency lines have been reported in the direction of NGC 2024 (Konovalenko 1984). We do not detect any lines in this direction. However, the observations of this direction were made in the daytime, under conditions of moderate interference. This is reflected by the rather large baseline parameter. It may also be noted that the T_{sys} was relatively low for this direction, although it should still be dominated by the antenna noise.

We observed 30 Doradus in the LMC because of the large quantities of interstellar material in the region. However, there is no strong source behind the LMC to illuminate this material, and no lines were detected in the velocity range from 0 to 500 km s^{-1}. Vela contains a strong source, but it is so close to the Sun that is is not surprising that no intervening line-producing region was found. G267.9−1.0, G287.4−0.6, and G327.3−0.6 are all molecular cloud complexes, but no lines were detected in their directions or in the G303.0+0.0 and G305.3+0.2 directions, which are the region of the Coalsack. (It is remarkable that we can detect no carbon lines in the Coalsack!)

G312.0+0.0 is a direction approximately tangent to the Scutum arm and, as shown in Figure 2, both α and β lines were found in this direction. This is a new detection. Beginning at $l = 340°$, lines were detected continuously along the plane to $l = 20°$, although the lines are rather weak between 340° and

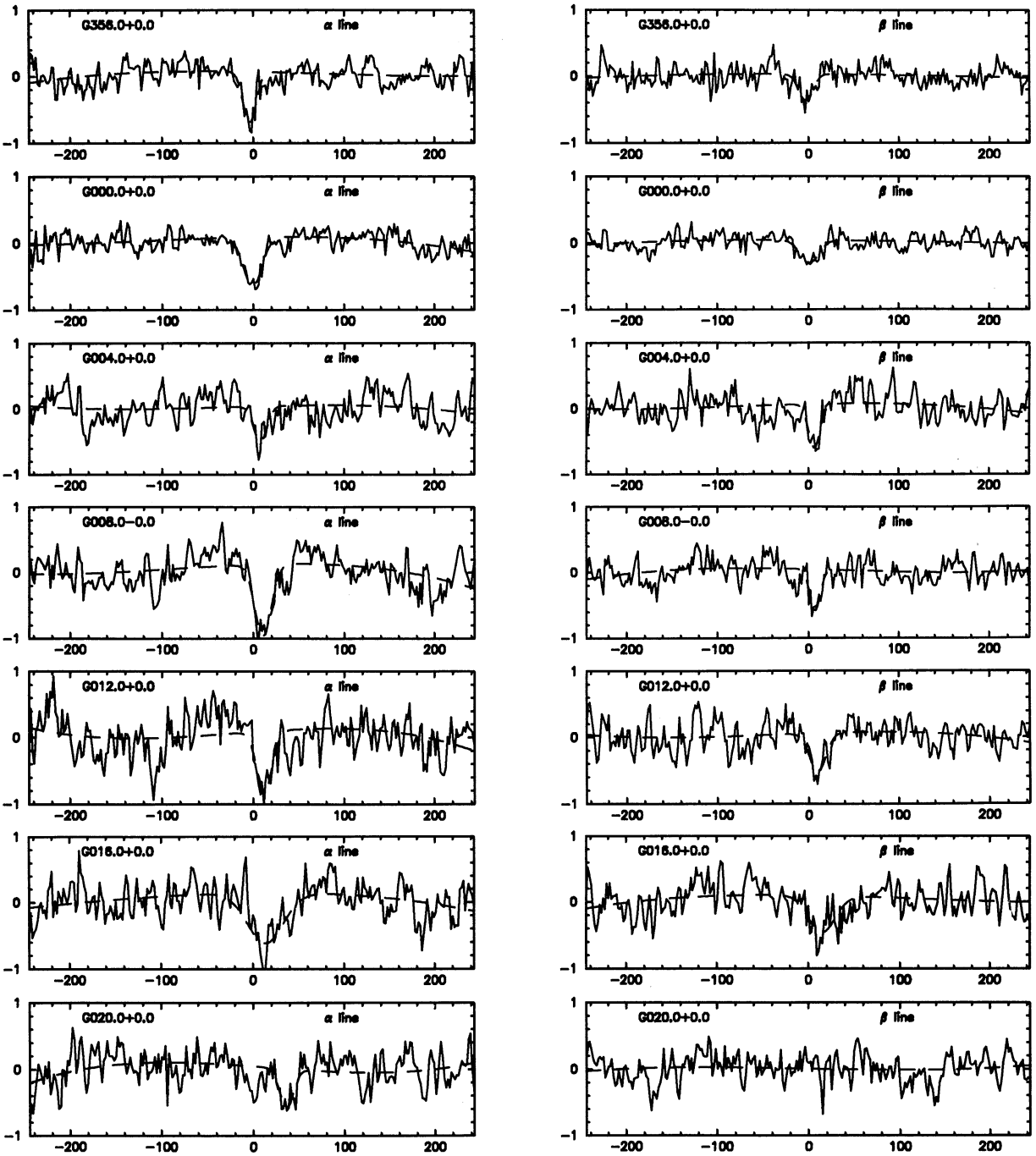

FIG. 2—*Continued*

346°. Therefore, there exists a very large line-forming region in these directions; it is spread over 40° in Galactic longitude. In order to estimate the extent of the region in Galactic latitude, some observations were made above and below the plane. At $b = \pm 2°$ (one-half beamwidth off the plane), the α-line depths appear to decrease substantially. However, the total line strengths, as indicated by the products of the line depths and widths, are essentially equal to those at $b = 0°$.

To obtain a higher signal-to-noise ratio in order to search for weak features, all the data with $b = 0°$ in the longitude range $352° < l < 8°$ were averaged together with the result shown in Figure 3. *The broadening of the lines caused by Galactic differential rotation over this range of longitude is negligible.* This fact is shown in Figure 4 by the similarity of the data averaged over three individual portions of this range: 352°–356°, 358°–002°, and 004°–008°.

The data were searched for the C635γ transition. A few of the fields, such as G312.0+0.0, G006.0+0, and G012.0+0.0, show small deflections at the expected γ-line frequencies, but there also exist deflections of similar magnitudes at other fre-

TABLE 1

CHARACTERISTICS OF THE OBSERVED LINES

			α-LINE			β-LINE			
FIELD (1)	TIME (1000 s) (2)	T_{sys} (K) (3)	T_L/T_{sys} ($\times 10^3$) (4)	ΔV (km s^{-1}) (5)	V_{lsr} (km s^{-1}) (6)	T_L/T_{sys} ($\times 10^3$) (7)	ΔV (km s^{-1}) (8)	V_{lsr} (km s^{-1}) (9)	D (kpc) (10)
NGC 2024	6.8	2129	(0.15)	...	...	(0.10)	...	...	...
30 Dor	18.6	2390	(0.16)	...	...	(0.08)	...	...	...
Vela.....	4.5	...	(0.10)	...	...	(0.07)	...	...	...
G267.9−1.0.....	9.0	3850	(0.13)	...	...	(0.07)	...	...	...
G287.4−0.6.....	13.2	4400	0.48(0.11)?	38(7)	−23	(0.12)	...	...	...
G303.0+0.0.....	12.0	4619	(0.11)	...	...	(0.08)	...	...	...
G305.3+0.2.....	11.1	5250	(0.07)	...	...	(0.07)	...	...	...
G312.0+0.0.....	6.0	6335	0.88(0.05)	16(1)	−53	0.65(0.09)	16(3)	−53	3.7
G327.3−0.6.....	9.0	8690	(0.08)	...	...	(0.08)	...	...	...
G336.0+0.0.....	18.9	9836	(0.08)	...	...	(0.11)	...	...	...
G338.0+0.0.....	6.0	9717	(0.09)	...	...	(0.09)	...	...	...
G340.0+0.0.....	9.0	9325	0.27(0.09)?	30(9)	−39	0.46(0.06)	31(4)	−40	3.1
G342.0+0.0.....	6.0	9276	0.53(0.06)?	17(2)	−39	(0.06)	...	...	3.2
G344.0+0.0.....	6.0	9922	0.65(0.07)	26(3)	−27	0.36(0.07)	30(6)	−34	2.7
G346.0+0.0.....	3.0	9686	0.20(0.11)?	20(13)	−20	(0.12)	...	...	1.8
G348.0+0.0.....	12.0	10108	0.53(0.09)	14(3)	−12	(0.08)	...	...	1.6
G350.0+0.0.....	3.0	9324	0.81(0.07)	14(2)	−11	0.36(0.07)	27(5)	−17	1.7
G352.0−2.0.....	3.0	8392	0.70(0.05)	23(2)	−17	0.69(0.10)?	11(3)	−2	3.0
G352.0+0.0.....	9.6	9702	1.25(0.08)	11(1)	−10	0.26(0.06)	12(4)	1	1.8
G352.0+2.0.....	3.0	8483	0.83(0.13)	22(4)	−8	0.29(0.06)	32(6)	−18	1.8
G354.0+0.0.....	3.0	10291	0.87(0.07)	26(2)	−10	0.25(0.13)?	21(13)	−6	2.4
G356.0+0.0.....	12.4	11891	0.76(0.05)	17(2)	−4	0.40(0.11)	18(6)	−3	1.7
G358.0−2.0.....	3.0	11300	0.53(0.11)	28(6)	−10	0.22(0.03)	26(4)	−10	...
G358.0+0.0.....	4.5	13210	0.90(0.11)	24(3)	−3	0.49(0.08)	24(4)	−5	...
G358.0+2.0.....	3.0	11598	0.80(0.15)	8(3)	3	(0.05)	...	...	...
G000.0−4.0.....	0.8	7910	0.33(0.11)?	13(6)	−6	(0.08)	...	...	...
G000.0−2.0.....	3.0	10640	0.57(0.07)	30(3)	−10	0.55(0.14)!	19(6)	−2	...
G000.0+0.0.....	26.1	15427	0.73(0.03)	24(1)	−1	0.35(0.03)	24(2)	1	...
G000.0+2.0.....	3.0	12386	0.70(0.10)	26(4)	−2	0.52(0.04)!	17(2)	−3	...
G000.0+4.0.....	3.0	7878	0.68(0.13)	31(5)	−2	0.83(0.09)!	5(2)	1	...
G002.0−3.5.....	6.0	...	0.52(0.12)?	5(3)	7	0.35(0.05)?	22(4)	6	...
G002.0−2.0.....	3.0	12247	0.97(0.08)	9(1)	5	0.75(0.04)	25(2)	3	...
G002.0+0.0.....	3.0	14154	0.90(0.05)	25(2)	2	0.68(0.07)!	12(2)	−1	...
G002.0+2.0.....	3.0	11828	0.61(0.10)	11(3)	6	0.64(0.07)	31(3)	0	...
G003.0+0.0.....	8.7	13010	0.90(0.07)	14(2)	−1	0.27(0.04)	19(3)	0	...
G004.0+0.0.....	6.0	12843	0.54(0.08)	17(3)	8	0.67(0.05)	15(2)	6	2.5
G006.0+0.0.....	7.5	12185	0.73(0.10)	25(4)	9	0.57(0.06)	22(3)	2	2.0
G006.6−0.2.....	4.5	11840	0.87(0.06)	28(2)	10	0.50(0.10)!	19(5)	5	2.1
G008.0+0.0.....	6.0	11546	1.09(0.10)	22(2)	11	0.63(0.06)!	14(2)	7	2.0
G010.0+0.0.....	6.3	10682	0.72(0.06)	26(2)	17	0.29(0.05)?	23(4)	13	2.4
G012.0+0.0.....	6.0	10225	0.91(0.07)	20(2)	12	0.59(0.06)	21(3)	10	1.5
G014.0−2.0.....	3.8	8127	0.88(0.09)	32(3)	11	0.46(0.06)	38(4)	16	1.4
G014.0+0.0.....	9.6	9970	0.85(0.10)	25(3)	16	0.37(0.05)	33(4)	18	1.8
G014.0+2.0.....	3.0	8483	0.51(0.12)	28(7)	21	0.62(0.07)	24(3)	16	2.0
G016.0+0.0.....	3.0	...	0.76(0.09)	47(4)	14	0.56(0.07)!	34(4)	15	1.7
G016.9+0.8.....	3.9	9350	1.07(0.06)	21(2)	20	0.71(0.07)!	15(2)	20	1.8
G018.0+0.0.....	3.0	9293	0.77(0.16)	33(6)	15	0.26(0.06)?	31(7)	21	1.4
G020.0+0.0.....	6.0	9148	0.59(0.08)?	18(3)	36	(0.10)	...	...	2.9
G022.0+0.0.....	4.6	9360	(0.10)	...	...	(0.11)	...	...	...
G024.0+0.0.....	6.0	8759	(0.06)	...	...	(0.07)	...	...	...

quencies. The averaged data were searched for this transition with a possible detection shown in Figure 3 and line parameters given in Table 2.

5. DISCUSSION

5.1. *Angular Distribution*

At $b = 0°$, the line strengths vary quite significantly at different longitudes, and they decrease abruptly beyond $l = \pm 20°$. This abrupt change is not caused by any abrupt change in the background radiation that illuminates the absorbing regions; the antenna temperatures vary smoothly through this range of longitude. The change must be the result of a decrease in the opacity of the absorbing region. Since we also find the lines when we observe along the Scutum arm at $l = 312°$, line-forming regions must also exist in other locations along the Sagittarius and/or Scutum arms. The distribution of the line-forming regions is obviously complex; a much more complete survey would be required to determine its characteristics.

As shown in Table 1, data were obtained at points above and below the plane only at $l = 352°$, 258°, 0°, 2°, and 14°, too few to permit any detailed modeling of the distribution in Galactic latitude. As mentioned above, the line strengths found at $b = \pm 2°$ are essentially the same as those at $b = 0°$. The

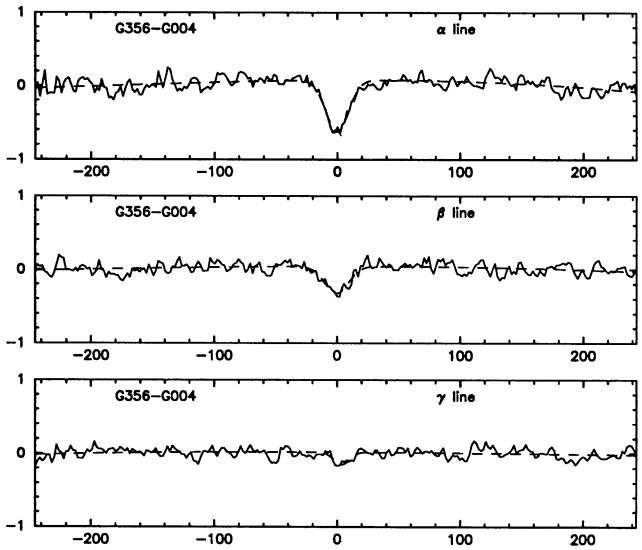

FIG. 3.—High-sensitivity profiles obtained by averaging all the data obtained at $b = 0°$ over the longitude range $352° < l < 8°$, where the smearing caused by differential rotation should be small. Abcissae and ordinates are the same as in Fig. 2. The characteristics of the fitted curves are in Table 2.

antenna temperatures fell significantly whenever we observed off the plane, indicating that the beam efficiency of the telescope was reasonably high. Thus, we conclude that the absorbing region must be approximately 4° wide in Galactic latitude. This means that, for the $b = 0°$ observations, the absorbing region must approximately fill the beam of the telescope, and the values given in Table 1 should not be greatly affected by beam dilution effects. At G000.0−4.0 and at G002.0−3.5 the lines appear to be very weak (note, however, that the G000.0−4.0 observations were disturbed by interference and have low sensitivity), while at G000.0+4.0 the line strengths are nearly equal to those at G000.0+0.0, so the distribution in latitude must be complicated.

TABLE 2

CHARACTERISTICS OF THE AVERAGED PROFILES

Field (1)	Line (2)	Time (1000 s) (3)	T_L/T_{sys} ($\times 10^3$) (4)	ΔV (km s^{-1}) (5)	V_{lsr} (km s^{-1}) (6)
G352−G008.....	α	91.1	0.65(0.04)	25(2)	1.0
G352−G008.....	β	91.1	0.37(0.04)	21(2)	0.8
G352−G008.....	γ	85.2	0.17(0.02)	15(2)	4.4

5.2. *Line Strength Ratios*

We consider first the line strength ratios between the α-lines and β-lines. Konovalenko (1990) asserts that this line strength ratio in the 76 MHz frequency range should be 1.5 over a wide range of anticipated physical conditions. The average ratio of line strengths, calculated as the ratio of the products of the line depth and width given in Table 1 and weighted according to observing time, is 2.06 ± 0.23. This estimate could be biased because we did not account for those cases in which the β-lines were not detected. However, an unbiased estimate, made using the data given in Table 2, also turns out to be 2.06. Our observed ratio appears to be significantly different from that given by Konovalenko, and it must be dependent upon physical conditions in the line-forming regions.

It is difficult to determine whether or not the line strength ratio between the α- and β-lines is constant or if it varies from field to field. The available evidence seems to favor the latter. The observed ratio varies from less than unity in some fields to more than four in other fields, a range that is well outside the formal errors derived from the least-squares fits to the lines. However, we should bear in mind that many of the fluctuations are not noiselike, and therefore the formal errors may only have a limited meaning. For instance, in those cases where the fields overlap by much less than a beamwidth, the ratios often disagree by more than their formal errors. Some of the apparently anomalous cases, where the observed width of the β-line is narrower than that of the α-line, may suggest that the α to β

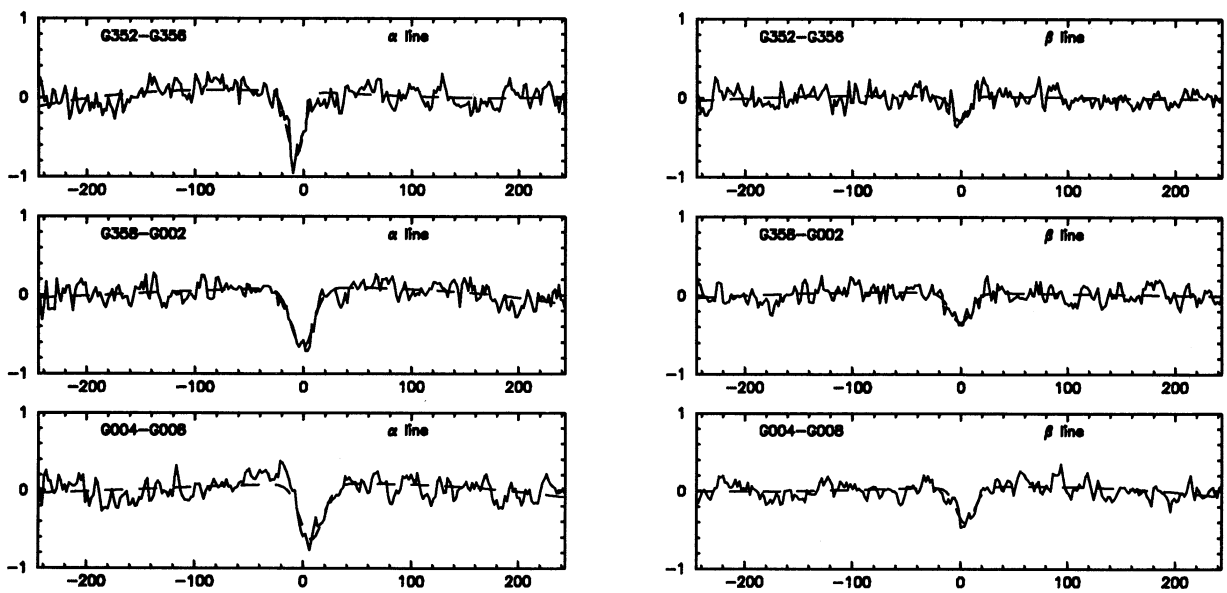

FIG. 4.—Profiles obtained at $b = 0°$ averaged over three longitude ranges. Abcissae and ordinates are the same as in Fig. 2.

line ratios are different for different clouds. As discussed below, the observed width of the lines is most likely the result of the presence of a number of clouds with different velocities within the telescope beam. If only a subset of these clouds produce the β-lines (owing to the differences in their line ratios), then the observed width of the β-line could be narrower.

The ratio of oscillator strengths between the 441α and 555β lines, as tabulated by Menzel (1969), is 5.75. Thus, the β-lines appear to be about $5.75/2.06 = 2.8$ times stronger than this oscillator strength ratio would predict. This presumably reflects the variation of the line strengths with principal quantum number and indicates that the C555α lines (which will occur at 38.4 MHz) are about 2.8 times stronger than the C441α lines at 76.4 MHz. If we accept the γ-line detection as being valid, a crude estimate of the line strength ratio is 6.27, while the oscillator strength ratio in this case is 16.29. This would suggest that the C635α lines (occurring at 25.6 MHz) would be about 2.6 times stronger than the C441α lines.

PAE94 have summarized the low-frequency recombination line data for the Perseus arm absorption in the direction of Cas A. Using the data given in Figure 11 of that paper, one finds that the ratio between the C555α and C441α line strengths is about 2.9. This compares well with the estimated ratio of 2.8 given above. From PAE94, one would also estimate the C635α to C441α ratio to be 4.5, while the crude estimate given above was 2.6. Thus, the available evidence indicates that the variation of line strength with frequency is fairly similar for the Perseus, Sagittarius, and Scutum arm regions and that the parameters of the line-forming model proposed by PAE94 for the Perseus arm region may also apply to the Sagittarius and Scutum arm regions.

5.3. *Line Widths*

Compared to the Perseus arm lines toward Cas A, which have widths of 6 to 7 km s^{-1} in the 75 MHz range (PAE89), the lines observed here are much wider with half-widths going up to 40 km s^{-1}. Since the widths of α- and β-lines, given in Table 1, are comparable in a majority of the cases, it is clear that the large line widths are not the result of pressure or radiation broadening; for pure pressure broadening, the C555β lines must be a factor of 3.3 wider than the C441α lines (Shaver 1975). The observed widths must therefore be largely due to Doppler broadening which, in velocity units, is independent of frequency or quantum number. If we assume that the pressure contribution to the C555β line is less than 10 km s^{-1} (a conservative upper limit), then the electron density in the line-forming regions must be less than 0.3 cm^{-3} for a temperature of 50 K.

Judging from the physical conditions deduced for the Perseus arm clouds (PAE94), the temperature of the line-forming regions is likely to be <75 K. Therefore, the contribution from thermal broadening to the line width is <2 km s^{-1}. In H I and molecular clouds, which are the likely sites for the formation of these lines, the line width resulting from internal turbulence is generally <3 km s^{-1}. The only other mechanism of Doppler broadening is differential Galactic rotation, which indeed can explain the observed line width if the line-forming clouds are distributed or extended along the line of sight. Deviations from circular motion, which are generally of the order of 5–10 km s^{-1} for H I clouds, could also contribute to the line width. Since the angular resolution of these observations is about 4°, a distribution of absorbing clouds both over the telescope beam and along the line of sight could generate the observed line width.

The line width measurement should be considered to be preliminary and require confirmation by further data. When we compared the data for those fields which were observed in both 1993 and 1994, the measured line widths were slightly larger in 1994. Also, Anantharamaiah et al. (1988) found line widths of about 15 km s^{-1} for G000.0+0.0 and for G016.9+0.8 (M16), while Table 1 gives values of 24 and 21 km s^{-1}, respectively. Although we tested the hardware and software systems carefully for any instrumental or environmental effects, it is possible that the lines were broadened by some undetected effect.

5.4. *Association with Other Components of the Interstellar Medium*

In Figure 5, we present a longitude-velocity diagram of the lines observed at $b = 0°$. The dots indicate the center velocity, and the horizontal lines indicate the half-width of the observed lines. The dotted and dashed lines in the diagram show the expected velocity for gas at Galactocentric radii of 5 kpc and 8 kpc, respectively, based on the rotation model given in Burton (1988). The observed gas appears to be confined to this range of Galactocentric distance through which there pass two spiral arms, the Sagittarius and Scutum arms (Georgelin & Georgelin 1976). The l-v diagram in Figure 5 bears only partial similarity to the l-v diagram of molecular clouds seen in ^{12}CO emission (e.g., Solomon & Sanders 1980) and even less similarity to the l-v diagram of neutral H I clouds seen in 21 cm emission (e.g., Burton 1988); both CO and H I lines extend over a much larger velocity range in these longitudes. On the face of it, this appears surprising, since for the Perseus arm clouds in the direction of Cas A, which have been studied in considerable detail (Anantharamaiah et al. 1994; PAE94), there seems to be a good correspondence between H I and carbon lines. This would imply either that the situation for Sagittarius and Scutum arms are very different from the Perseus arm or that there is a selection effect. We favor the latter possibility. Two factors could contribute to the difference in the velocity structure between 21 cm H I lines and the low-frequency carbon

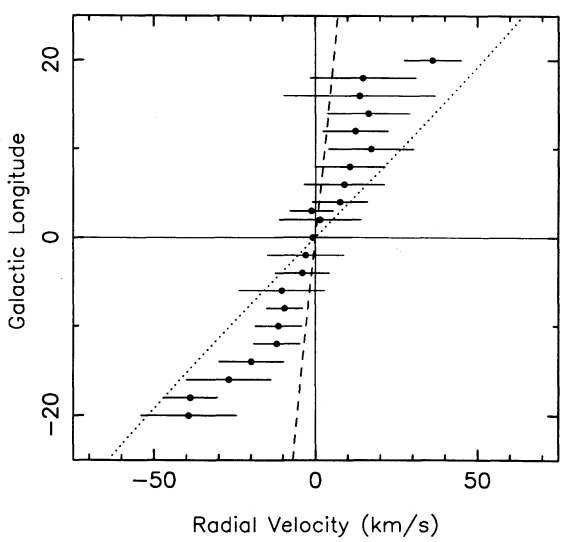

FIG. 5.—Longitude-velocity diagram of the carbon recombination lines observed at $b = 0°$. Dots indicate the center velocity, and horizontal lines indicate the half-width of the lines. Dotted and dashed curves show the expected variation for gas at Galactocentric radii of 5 kpc and 8 kpc, respectively.

recombination lines. First, the carbon lines, which are seen in absorption against the Galactic nonthermal background, are more easily observed from nearby gas for which the intensity of the background radiation is larger and beam dilution is smaller and second, only the cooler H I concentrations will contribute to the carbon lines, since the integrated optical depth of the recombination lines goes as $T^{-2.5}$. *The cooler H I concentrations may show up as self-absorption in 21 cm line profiles but be difficult to identify in an l-v diagram.* Given these selection effects, it is not surprising that there is no one-to-one correspondence between the velocity distribution of carbon recombination lines and 21 cm H I lines, although both lines could arise in neutral H I clouds in the interstellar medium (ISM) as argued by PAE94.

5.5. *Other Low-Frequency Lines*

We consider what other lines may possibly be found in the data. The most significant profiles in the respect are in Figures 3 and 4, in which the data have been averaged over intervals of longitude to increase signal-to-noise ratios. In each of these profiles, the hydrogen recombination line, if present, would appear at a frequency 38.10 kHz below the carbon line frequency, i.e., at a velocity of $+149.4$ km s^{-1} with respect to the carbon line. To a level of $T_L/T_{sys} < 10^{-4}$, there is no trace of hydrogen recombination lines. Aside from the carbon lines, the only significant feature in the profiles is a broad depression about 40 km s^{-1} in half-width centered at -180 km s^{-1}. This feature seems to appear in both the α-line and β-line profiles. It is not associated with the "3 kpc arm" which crosses $l = 0°$ at -53 km s^{-1}. It is more tempting to associate it with features at similar velocities on CO and CS maps of the Galactic center region (Blitz et al. 1993). However, the CO and CS features appear only in the $-2° < l < 0°$ range, while Figure 4 indicates that the -180 km s^{-1} feature appears at both positive and negative longitudes and is much more extensive than the CO/CS feature. It should be noted that a -180 km s^{-1} feature cannot be generated by other atomic or molecular species. Recombination lines from atoms lighter than carbon would occur at lower frequencies, i.e., positive velocities, with respect to the carbon lines. Recombination lines from heavier atoms would occur indistinguishably near the carbon lines.

The G000.0+0.0 data were also searched for any features at the positronium recombination line frequencies. Although positronium is known to exist in this direction (Purcell et al. 1993), the expected population of high quantum number states is too small to produce any detectable recombination lines (Anantharamaiah et al. 1993) and, indeed, no positronium lines were found. The baseline parameter (as in Table 1) for this observation was 0.099, and the upper limit for any positronium α-lines was $T_L/T_{sys} < 2 \times 10^{-4}$.

6. CONCLUSIONS

This initial survey of the southern portion of the Galactic plane has revealed 76 MHz carbon absorption lines formed in a very extended region from $l = 340°$ to $l = 20°$ and several degrees wide in Galactic latitude. The C441α lines and C555β lines were both well observed. Kinematic distances, deduced from the center velocity and width of the lines, place this region in the nearby Sagittarius and/or Scutum arms. This is the first such extended region to be found, but it seems probable that similar regions may exist in other directions and that they may be a fairly common feature of the ISM. Our detection was facilitated by good system sensitivity combined with strong Galactic background emission which illuminated the absorbing region.

A comparison of α and β line strengths suggests that the variation of line strength with principal quantum number may be similar to that found for the Perseus arm absorption region in the direction of Cas A. The line widths are larger and appear to be contributed by Galactic differential rotation. The data were searched for recombination lines generated by other atomic species, especially hydrogen, but none were found.

This work was partially supported by the National Science Foundation under grant AST 92-00831. The construction of the feed system was carried out at Parkes with the enthusiastic collaboration of the workshop staff. We also want to thank all of the observatory staff for their cheerful acceptance of the many inconveniences that resulted from the fact that we needed to turn off all nonessential power in order to eliminate interference to our observations.

REFERENCES

Anantharamaiah, K. R., Dwarakanath, K. S., Morris, D., Goss, W. M., & Radhakrishnan, V. 1993, ApJ, 410, 110
Anantharamaiah, K. R., Erickson, W. C., Payne, H. E., & Kantharia, N. G. 1994, ApJ, 430, 682
Anantharamaiah, K. R., Payne, H. E., & Erickson, W. C. 1988, MNRAS, 235, 151
Blake, D. H., Crutcher, R. M., & Watson, W. D. 1980, Nature, 287, 707
Blitz, L., Binney, J., Lo, K. Y., Balley, J., & Ho, P. T. P. 1993, Nature, 361, 417
Burton, W. B. 1988, Galactic and Extragalactic Radio Astronomy-Second Edition, ed. G. L. Verschuur & K. I. Kellermann (New York: Springer-Verlag), 295
Georgelin, Y. M., & Georgelin, Y. P. 1976, A&A, 49, 57
Golynkin, A. A., & Konovalenko, A. A, 1990, in Radio Recombination Lines: 25 Years of Investigation, ed. M. A. Gordon & R. L. Sorochenko (Dordrecht: Kluwer), 209
Konovalenko, A. A. 1984, Soviet Astron. Lett., 10, 384
Konovalenko, A. A. 1990, in Radio Recombination Lines: 25 Years of Investigation, ed. M. A. Gordon & R. L. Sorochenko (Dordrecht: Kluwer), 175
Konovalenko, A. A., & Sodin, L. G. 1980, Nature 283, 360
Menzel, D. H. 1969, ApJS, 18, 221
Payne, H. E., Anantharamaiah, K. R., & Erickson, W. C. 1989, ApJ, 341, 890 (PAE89)
———. 1994, ApJ, 430, 690 (PAE94)
Purcell, W. R., Grabelsky, D. A., Ulmer, M. P., Johnson, W. N., Kinzer, R. L., Kurfess, J. D., Strickman, M. S., & Jung, G. V. 1993, ApJ, 413, L85
Shaver, P. A. 1975, Pramana, 5, 1
Solomon, P. M., & Sanders, D. B. 1980, in Giant Molecular Clouds in the Galaxy, ed. P. M. Solomon & M. G. Edmunds (Oxford: Pergamon), 41
Watson, W. D., Western, L. R., & Christensen, R. B. 1980, ApJ, 240, 956
Wong, J. L., & King, H. E. 1990, Report No. TR-0073(3404)-2, Aerospace Corp., El Segundo, CA